Vu Thi Lan Anh
Doctor of Philosophy (PhD)
Hanoi University of Mining and Geology, Vietnam
Nguyen Phuong Dong
PhD in Geography
Hanoi University of Mining and Geology, Vietnam
Nguyen Thi Hong
Master, lecturer
Hanoi University of Mining and Geology, Vietnam

ASSESSMENT OF OIL SPILL IMPACTS AND DISPERSION ASSOCIATED WITH RIVER SAND MINING: A CASE STUDY IN THE LOWER RED RIVER, VIETNAM

Abstract*: River sand mining relies on dredging vessels, pumps, generators, and waterborne transport, creating a potential risk of oil leakage and spills directly into the aquatic environment. This study assesses potential spill sources, hydrodynamic conditions, oil dispersion, and environmental impacts associated with an oil-spill scenario at a sand mine in the lower Red River. Flow conditions were surveyed using an Acoustic Doppler Current Profiler (ADCP) at seven cross-sections. The hydrodynamic model employed an unstructured mesh with element sizes of approximately 10–30 m, refined to about 10 m within the mining area. Cross-sectional mean velocities ranged from approximately 0.20 to 0.26 m/s, with discharges of 621.65–1,056.46 m³/s. Simulations of the existing and post-mining conditions indicated only minor changes in water level, whereas localized changes occurred in flow velocity and direction. The worst-case scenario assumed that the entire daily diesel oil (DO) demand of 1,036.5 L was continuously released over 24 h, equivalent to approximately 922.5 kg/day and 38.44 kg/h, with particle trajectories updated at 5-min intervals. The oil slick was initially concentrated around the source and subsequently elongated along*

the prevailing flow direction over 30–120 min. The results highlight the importance of the flow field, surface wind, oil properties, and release rate in predicting oil trajectories and planning spill-response measures.
Keywords: sand mining; oil spill; dispersion modeling; environmental risk.

1. INTRODUCTION

River sand mining supplies essential construction materials but may alter bed morphology, velocity distribution, flow direction, and bank stability. In addition to morphological and hydraulic impacts, dredging vessels and mechanical equipment pose risks of oil contamination through fuel-system leakage, refueling, maintenance activities, tank damage, or vessel accidents. Previous studies on in-channel aggregate extraction have shown that bed lowering can induce hydraulic and morphological changes ranging from local effects to river-reach-scale responses (Kondolf, 1997; Rinaldi et al., 2005; Koehnken & Rintoul, 2018).

Once released into the aquatic environment, oil is simultaneously affected by spreading, advection, diffusion, evaporation, dissolution, dispersion, oxidation, oil–particle interactions, and biodegradation (National Research Council, 2003; Spaulding, 2017; Reed et al., 1999; Fingas, 2017; Lee et al., 2015; Gong et al., 2014). For diesel oil, aromatic hydrocarbons and oil associated with suspended particulate matter may be toxic to aquatic organisms and can ultimately be transferred to sediments (Fingas, 2017; Incardona et al., 2004; Carls et al., 1999; Barron et al., 2004; Peterson et al., 2003). Oil-trajectory modeling is therefore an important tool for predicting affected areas, estimating arrival times at sensitive receptors, and allocating spill-response resources (Spaulding, 2017; Reed et al., 1999; ITOPF, 2014).

Although research on river sand mining has largely focused on channel morphology, hydrodynamics, bank erosion, and water quality, the risk of oil spills from vessels and mining equipment operating directly on rivers has received comparatively limited attention from a dispersion-modeling perspective. In particular, mining-induced changes in the flow field may modify the direction and spatial extent of oil transport during an accidental release. Integrating hydrodynamic modeling with oil-spill simulation is therefore useful for delineating potentially affected areas and supporting environmental emergency-response planning.

2. RESEARCH METHODOLOGY

2.1. Study area

The sand mine covers approximately 3.92 ha and is located in the lower Red River in the Nam Tien Hai area.

2.2. ADCP flow survey

Flow was measured at seven cross-sections: MC1–MC2 upstream, MC3–MC5 within the mining area, and MC6–MC7 downstream (Figure 1). Measurements were obtained using an Acoustic Doppler Current Profiler (ADCP), which provides velocity distributions over depth and across a cross-section and is well suited to large rivers and tidally influenced environments (Simpson & Oltmann, 1993; Mueller et al., 2013).

Figure 1. Locations of the surveyed cross-sections

Table 1. Summary of hydrological survey data for the mining area

Cross-section	Cross-section width B (m)	Wetted cross-sectional area F	Mean cross-sectional velocity	Discharge Q (m³/s)	Maximum depth Hmax (m)

		(m²)	Vmean (m/s)		
MC1	358.91	4,136.56	0.26	621.65	16.12
MC2	269.40	3,195.54	0.20	634.99	14.62
MC3	343.44	3,621.11	0.20	708.12	13.12
MC4	348.28	3,726.06	0.20	755.98	12.12
MC5	387.91	4,020.81	0.22	883.33	11.62
MC6	400.08	3,978.48	0.26	1.046.95	11.62
MC7	358.91	4,136.56	0.26	1.056.46	14.12

The velocity distributions across selected cross-sections are shown below:

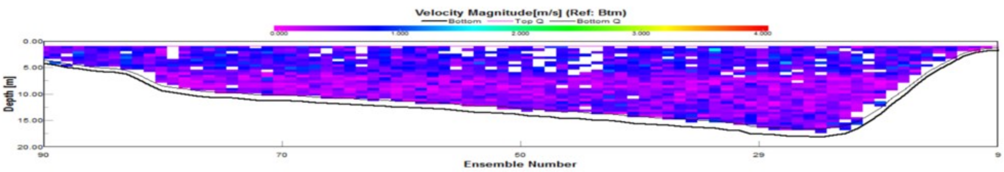

Figure 2. Flow velocity distribution across cross-section MC1

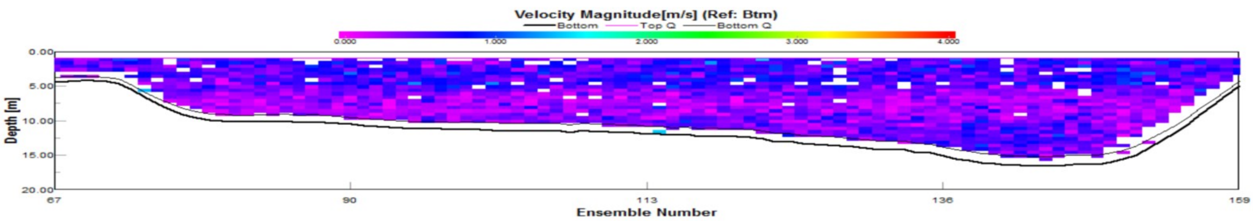

Figure 3. Flow velocity distribution across cross-section MC2

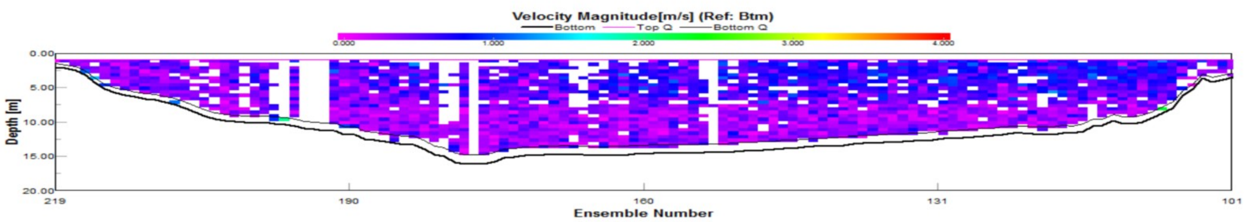

Figure 4. Flow velocity distribution across cross-section MC7

2.3. Hydrodynamic model

The model is based on the Reynolds-averaged Navier–Stokes equations for an incompressible fluid, together with the Boussinesq approximation and hydrostatic-pressure assumption. The horizontal domain was discretized using an unstructured mesh with element sizes of approximately 10–30 m and refined to about 10 m within the mining area. Two scenarios were compared: the existing bathymetry and the post-mining bathymetry with a lowered bed elevation, both subjected to representative flood conditions associated with Typhoon Yagi in September 2024. Flexible-mesh hydrodynamic modeling is well suited to river–estuary systems with complex geometries (DHI, 2017; Hervouet, 2007).

2.4. Oil-spill scenario

The total diesel oil demand of the mining operation is 1,036.5 l/day. Assuming a density of 0.89 kg/L, this corresponds to approximately 922.5 kg/day. The adverse scenario assumes that the entire amount is released continuously over 24 h from a source located near the center of the mining area, corresponding to a release rate of approximately 38.44 kg/h. Trajectories were updated at 5-min intervals and analyzed at 0, 30, 60, and 120 min. Key oil-model inputs include oil type and quantity, release rate, currents, tides, wind, and temperature (Spaulding, 2017; Reed et al., 1999; French-McCay, 2004).

3. RESULTS AND DISCUSSION

3.1. Hydrodynamic characteristics

The surveyed cross-sections were approximately 269–400 m wide. Cross-sectional mean velocities ranged from 0.20 to 0.26 m/s, while measured discharges ranged from 621.65 to 1,056.46 m^3/s. Velocity distributions varied over both depth and channel width, reflecting the influence of channel morphology, tidal forcing, and local flow structures.

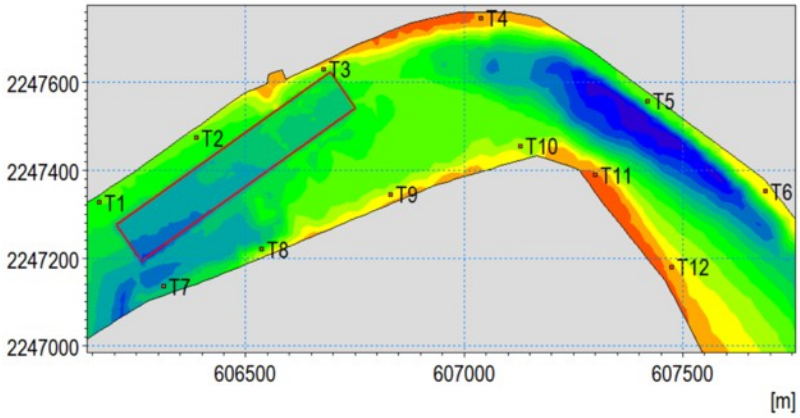

Figure 5. Locations of model-output extraction points

Water level:

Within the study area, including both the left and right banks, the simulations indicate that water levels remain virtually unchanged relative to the existing condition. Water-level variations at the monitoring points are very small, generally ranging from −0.002 to 0.006 m. Along the left bank, most monitoring points from T1 to T6 show mean water-level differences of zero or near zero, indicating no localized water-level rise along the bank. At T3, a slight increase is observed, with a mean value of approximately 0.004 m. This is mainly attributable to the change in bed morphology after lowering the bed elevation, which modifies the local flow distribution and produces slight water accumulation near the mining area. However, this increase is negligible. Similarly, along the right bank, water levels at T7–T12 after mining are nearly identical to those under existing conditions, with mean differences of approximately ±0.001 m. T9 and T10 also show very small, localized, and intermittent increases.

Flow velocity:

- Reach 1 (T1–T3): This bank segment runs parallel to the longitudinal boundary of the mining area. The simulations show a slight decrease in flow velocity after bed lowering compared with the existing condition. Mean velocity decreases by approximately 0.026 m/s at T1, 0.060 m/s at T2, and 0.081 m/s at T3. The time series indicate that these reductions are most pronounced during strong flood- and ebb-tidal phases. The principal reason is that bed lowering locally enlarges the flow cross-section, disperses flow energy, and reduces near-bank current intensity.

- Reach 2 (T4–T6): This bank segment is located downstream of the mining area. At these points, flow velocity increases slightly after mining during some periods of strong tidal flow, with mean increases of approximately 0.005 m/s at T4, 0.003 m/s at T5, and 0.002 m/s at T6.

- The overall pattern of velocity variation is similar to that along the left bank, but the magnitude of change is smaller. At T7–T10, post-mining velocities are only slightly lower, with mean reductions ranging from 0.013 to 0.041 m/s. The decrease is stable and no abrupt periods of velocity increase are observed.

- At T11 and T12, the velocity time series for the two scenarios are nearly coincident, with only very small increases (below 0.004 m/s).

Flow direction:

Changes exceeding 1° are observed at several locations, notably T1, T3, and T11. At T3, the mean flow direction decreases by approximately 1.64°, indicating that the current becomes more oblique toward the bank than under existing conditions. This location warrants attention because such a directional change may increase the risk of localized bank erosion. At T11, the mean flow direction increases by approximately 2.28°; however, this point is farther from the mining area and the directional change is not accompanied by an increase in velocity, so the potential adverse impact is limited. The remaining locations show no substantial change in flow direction.

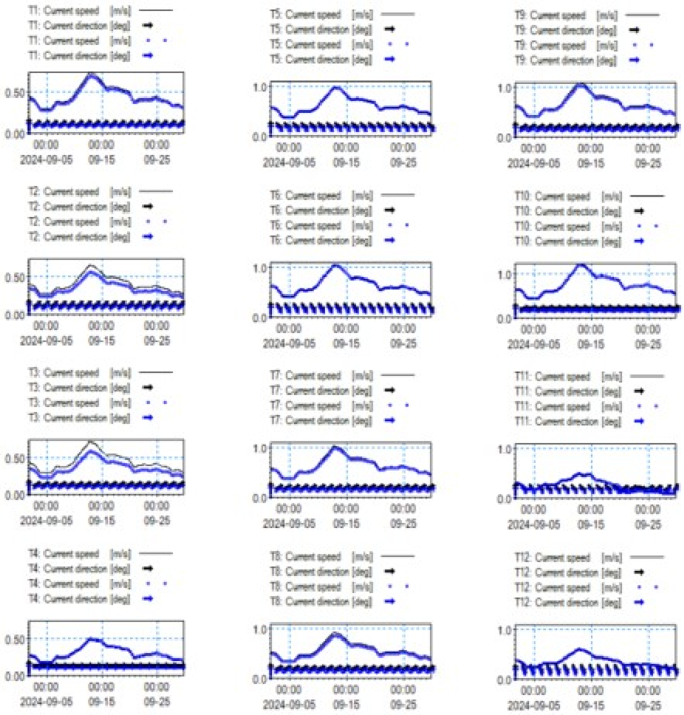

Figure 6. Time series of flow velocity at 12 bank-side points

3.2. Mining-induced changes in the flow field

Water-level differences between the two scenarios were generally between −0.002 and 0.006 m. Along the left bank, mean velocity at T1–T3 decreased by approximately 0.026–0.081 m/s, whereas T4–T6 showed slight increases of about 0.002–0.005 m/s. Along the right bank, velocities at T7–T10 decreased by approximately 0.013–0.041 m/s, while changes at T11–T12 were very small. Changes in flow direction were below 1° at most locations; however, the mean direction at T3 decreased by approximately 1.64°, while that at T11 increased by about 2.28°. Thus, bed lowering did not substantially alter the overall water-level regime but could locally redistribute flow velocity and direction.

3.3. Oil-spill dispersion

At the onset of the release, oil was concentrated around the source. After 30 min, the slick elongated along the principal flow direction but remained largely within the mining area and adjacent waters. After 60 min, its spatial extent increased. By 120 min, the slick formed a relatively continuous band along the near-bank current, while oil density near the source decreased as the oil was advected and dispersed. This evolution is consistent with oil-trajectory behavior that is initially controlled by currents and wind while simultaneously undergoing weathering processes (National Research Council, 2003; Spaulding, 2017; Reed et al., 1999).

The simulation indicates that under a continuous release at a relatively low rate (38.44 kg/h), the slick does not develop abruptly at high density; rather, it forms and spreads progressively over time, directly controlled by the prevailing current regime and surface wind at the time of the incident.

At the onset of the incident (Figure 7), the amount of newly released oil is small relative to the transport capacity of the flow; consequently, the oil remains concentrated mainly around the spill source. The affected area is still limited, and the oil has not yet spread widely into surrounding waters.

After 60 min (Figure 9), as oil continues to enter the environment, the spatial extent of the slick increases more clearly. The slick is transported along the prevailing flow direction. Although the affected area expands, oil density within individual areas tends to decrease because the oil is advected and dispersed over a larger area.

After 120 min (Figure 10), the slick forms a relatively continuous band along the near-bank flow direction. Oil density near the source gradually decreases as the oil is transported and dispersed spatially.

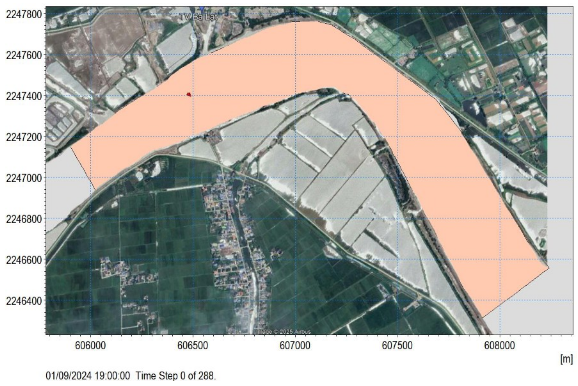

Figure 7. Oil slick location at the onset of the spill

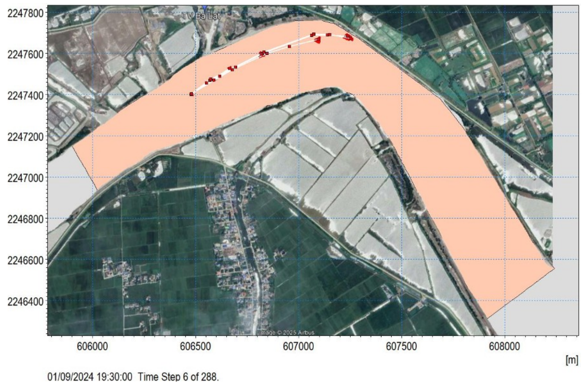

Figure 8. Oil spill trajectory 30 minutes after the onset of the spill

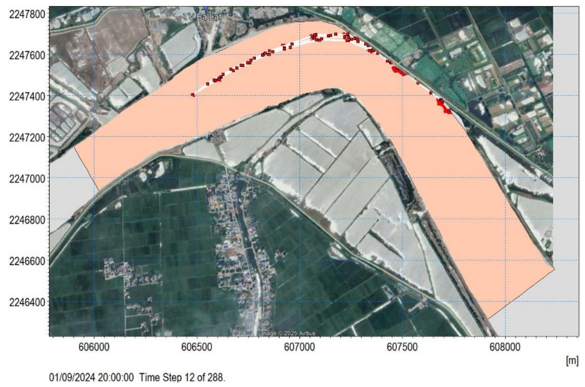

Figure 9. Oil spill trajectory 60 minutes after the onset of the spill

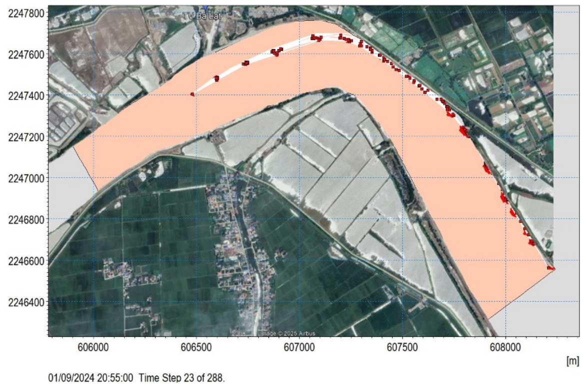

Figure 10. Oil spill trajectory 120 minutes after the onset of the spill

3.4. Discussion

During dispersion, a decrease in oil density at the water surface does not imply that the oil has been completely removed from the environment. A fraction may evaporate, dissolve, or disperse into the water column, while the remainder may undergo oxidation and biodegradation or become associated with suspended particles and settle to the bed (National Research Council, 2003; Fingas, 2017; Lee et al., 2015; Gong et al., 2014). In sand-mining areas, dredging and sand unloading disturb sediments and may increase suspended-solid concentrations. Consequently, oil may adhere to these particles and accumulate in bottom sediments (Lee et al., 2015; Gong et al., 2014).

Diesel oil contains numerous hydrocarbon constituents that can adversely affect aquatic organisms. In particular, some polycyclic aromatic hydrocarbons (PAHs) may cause toxicity and impair fish development, physiological function, and reproduction (Incardona et al., 2004; Carls et al., 1999; Barron et al., 2004; Peterson et al., 2003). Eggs and larvae are generally more sensitive to oil contamination than adult fish. For benthic organisms, effects may persist when oil associates with suspended matter, settles, and accumulates in sediments.

The simulation shows that the slick was transported predominantly by the flow field during the first 120 min, consistent with Reed et al. (Reed et al., 1999) and Spaulding (Spaulding, 2017), who emphasized the dominant role of the velocity field in controlling oil trajectories during the early stage of a spill.

However, because post-mining changes in flow velocity and direction in the study area were relatively small, the influence of bed lowering on the oil trajectory was primarily local.

CONCLUSIONS

This study integrated ADCP observations, hydrodynamic modeling, and an oil-spill scenario to assess spill risk at a river sand mine. Surveys at seven cross-sections showed mean velocities of 0.20–0.26 m/s and discharges of 621.65–1,056.46 m^3/s. Bed lowering had little effect on the overall water level but produced localized changes in flow velocity and direction. Under the scenario in which 1,036.5 L of diesel oil per day was released continuously over 24 h, the modeled source rate was approximately 38.44 kg/h, and the slick was clearly transported by the flow field during the first 30–120 min. The results indicate that mining-induced changes in velocity and flow direction are primarily local, whereas water levels remain nearly unchanged. Under the hypothetical spill scenario, the flow field controls the direction of oil transport during the first 120 min, causing the slick to extend downstream along the riverbank. Oil-spill risk assessment for river sand mining should therefore integrate hydrodynamic conditions, spill-source location, and sensitive downstream receptors. These results can support the delineation of priority response zones and the strategic placement of oil-spill containment and control equipment at river sand-mining sites.

Acknowledgements

The authors thank the HUMG project “Research on the impact of sand mining activities in the Tra Ly River area, Hung Yen Province using the MIKE21SW – HD – MT model” under Project Code: T26-38.

REFERENCES

1. Kondolf, G.M. (1997). Hungry water: Effects of dams and gravel mining on river channels. Environmental Management, 21, 533–551.

2. Rinaldi, M., Wyzga, B., & Surian, N. (2005). Sediment mining in alluvial channels: Physical effects and management perspectives. River Research and Applications, 21, 805–828.
3. Koehnken, L., & Rintoul, M.S. (2018). Impacts of Sand Mining on Ecosystem Structure, Process and Biodiversity in Rivers. WWF.
4. National Research Council. (2003). Oil in the Sea III: Inputs, Fates, and Effects. National Academies Press..
5. Spaulding, M.L. (2017). State of the art review and future directions in oil spill modeling. Marine Pollution Bulletin, 115, 7–19.
6. Reed, M., Johansen, Ø., Brandvik, P.J., Daling, P., Lewis, A., Fiocco, R., Mackay, D., & Prentki, R. (1999). Oil spill modeling towards the close of the 20th century: Overview of the state of the art. Spill Science & Technology Bulletin, 5, 3–16.
7. Fingas, M. (Ed.). (2017). Oil Spill Science and Technology. Elsevier.
8. Lee, K., Boufadel, M., Chen, B., Foght, J., Hodson, P., Swanson, S., & Venosa, A. (2015). Expert Panel Report on the Behaviour and Environmental Impacts of Crude Oil Released into Aqueous Environments. Royal Society of Canada.
9. Gong, Y., Zhao, X., Cai, Z., O'Reilly, S.E., Hao, X., & Zhao, D. (2014). A review of oil, dispersed oil and sediment interactions in the aquatic environment. Marine Pollution Bulletin, 79, 16–33.
10. Incardona, J.P., Collier, T.K., & Scholz, N.L. (2004). Defects in cardiac function precede morphological abnormalities in fish embryos exposed to polycyclic aromatic hydrocarbons. Toxicology and Applied Pharmacology, 196, 191–205.
11. Carls, M.G., Rice, S.D., & Hose, J.E. (1999). Sensitivity of fish embryos to weathered crude oil: Part I. Environmental Toxicology and Chemistry, 18, 481–493.

12. Barron, M.G., Carls, M.G., Heintz, R., & Rice, S.D. (2004). Evaluation of fish early life-stage toxicity models of chronic embryonic exposures to complex PAH mixtures. Toxicological Sciences, 78, 60–67.
13. Peterson, C.H., Rice, S.D., Short, J.W., Esler, D., Bodkin, J.L., Ballachey, B.E., & Irons, D.B. (2003). Long-term ecosystem response to the Exxon Valdez oil spill. Science, 302, 2082–2086.
14. ITOPF. (2014). Fate of Marine Oil Spills. Technical Information Paper 2.
15. Simpson, M.R., & Oltmann, R.N. (1993). Discharge-Measurement System Using an Acoustic Doppler Current Profiler with Applications to Large Rivers and Estuaries. USGS Water-Supply Paper 2395.
16. Mueller, D.S., Wagner, C.R., Rehmel, M.S., Oberg, K.A., & Rainville, F. (2013). Measuring Discharge with Acoustic Doppler Current Profilers from a Moving Boat. USGS Techniques and Methods 3-A22.
17. DHI. (2017). MIKE 21 & MIKE 3 Flow Model FM: Hydrodynamic and Transport Module, Scientific Documentation.
18. Hervouet, J.-M. (2007). Hydrodynamics of Free Surface Flows: Modelling with the Finite Element Method. Wiley.
19. French-McCay, D.P. (2004). Oil spill impact modeling: Development and validation. Environmental Toxicology and Chemistry, 23, 2441–2456.
20. National Academies of Sciences, Engineering, and Medicine. (2022). Oil in the Sea IV: Inputs, Fates, and Effects. The National Academies Press.